Lasers in Manufacturing Conference 2019

Periodic structures for superhydrophobic performance of metallic surfaces produced by femtosecond pulsed laser

P.W. Butler-Smith[a,b] ,T.L See[a], J. Liu[b], X. Hou[b]

[a]*Manufacturing Technology Centre (MTC), Ansty Park, Coventry, CV7 9JU, UK*
[b]*The University of Nottingham, University Park, Nottingham NG7 2RD, UK*

Abstract

Superhydrophobic surfaces can be defined as those exhibiting a water contact angle of greater than 150° with high water droplet mobility. Such surfaces typically benefit from air pockets formed under incident water droplets which are partially suspended by hierarchical structures of acutely angled protruding micro-asperities. In this work, controlled populations of regular pyramid structures measuring less than 100 micrometres across were formed in aluminium substrates in defined patterns using a femtosecond pulsed laser. It has been demonstrated from the as-processed surfaces that the water droplet contact angle was dependent on feature population, escalating to a level of superhydrophobicity, with water contact angles up to 157° and roll off angle of as low as 2° being achieved. In addition, investigations were undertaken on these laser processed surfaces on performance consistency and durability with the view to upscale for applications in the aerospace, energy, medical, food and wider industrial sectors.

Keywords: Femtosecond laser, hydrophobic, contact angle, periodic structures,

1. Introduction

The fabrication of super-hydrophobic surfaces exhibiting self-cleaning properties is particularly attractive for an extensive range of applications such as surface coatings, fabricated panels, windows and fabrics. It is well established that naturally occurring surface hydrophobicity (e.g. lotus leaf) is achieved from a combination surface roughness, defined by specific arrangements of protruding geometric asperities, the prevailing chemistry of the surface and the contact water droplet as reported by Barthlott and Neinhuis, 1997. Hydrophobic interactions are also governed by factors such as temperature, pressure, surface charge energy and liquid borne impurities, reported by Jungwirth and Cremer, 2014. It was established by Wenzel, 1936 that the fluid incident on surface asperities can also wet the associated depressions between asperities, thereby leading to an increase in the wettable contact area of a surface. This was accounted for by including a roughness factor r in Young equation,

* Corresponding author. Tel.: +44 7796 445 600.
E-mail address: Paul.Butler-Smith@nottingham.ac.uk

$$\cos \Theta^{l} = r \cos \Theta \quad [1]$$

where r corresponds to the apparent contact angle Q^{l}, for a contact angle Q of an equivalent flat surface. The ratio of the incident surface and the projected wettable surface areas thereby provides a measure of water droplet retention.

By contrast, Cassie and Baxter, 1994 claimed that a droplet is suspended only on the tips of protruding asperities without filling the associated depressions between them. Therefore suspension is effected by an equivalent flat surface contact area and the ambient air contained within the depressions and is defined by the fractional areas of the asperities and air cushions. The contact angle Θ^{l} is therefore an average between the contact angle on the surface Θs and on air Θv (= 180^{0}) and is given by

$$Q^{l} = -1 + \Phi s\,(1 + \cos Q) \quad [2]$$

where Φs is the fractional area of the wetted material asperities. The Cassie Baxter equation thus offers a measure of rejection of the water droplet.

It has subsequently been shown by Gao et. al., 2009, Extrand and Kumagai, 1997, that the surface morphology close to the contact line determines the contact angle and hysteresis of the water droplet, therefore indicating that the geometry of the asperities influences the contact angle. Furthermore, surfaces consisting of hierarchical structures have been reported by Gao and Mccarthy, 2006, to produce superior hydrophobic performance.

A number of methods on the fabrication of artificial superhydrophobic surfaces, using for instance, chemical or electrochemical deposition, lithography and plasma based processes have been reported by Shirtcliffe, 2008. Of these, laser based processes offer significant advantages in the production of designed micro-textures having geometric uniformity and distribution of the required asperities to achieve superhydrophobic performance, as recorded by Luo et. al., 2010, Tang et. al., 2008, Kietzig, 2009.

The flexibility of laser processing also offers the potential of producing site-specific textures exhibiting hydrophobic and hydrophilic performance as presented by Kim and Noh, 2018. This study explores the application of laser processing for the production of textures on metallic substrates to produce controlled levels of hydrophobicity and the performance durability through accelerated surface aging.

2. Laser processing of hydrophobic surfaces

A study was undertaken to evaluate the effects of both texture design and feature population on hydrophobic performance of an EN40 steel and a commercial grade aluminium substrates. Two distinctly different texture designs were selected, one based on dimples of specific area ratios and the other predominated by defined populations of columnar aspirates.

2.1. Dimpled texturing – nanosecond pulsed laser

Non-staggered arrays of dimples on 10mm x 10mm sites were produced in precut flat EN40 steel plates using an AgieCharmilles 600 5Ax fibre optic nanosecond pulsed laser system by Georg Fischer Machining Solutions. A cross-hatch scanning path was used for the laser parameters as given in Table 1. Five area ratios (AR), defined by a unit planar processed area to the overall unit area, were produced from AR = 5% to 50%. The produced dimples were measured using an Alicona G4 Focus Variation microscope. The dimples exhibited a nominal diameter of 120µm and a nominal depth from the original surface of 15µm. Each dimple

was characterised by recast material, forming an irregular crown immediately around the dimple perimeter having a nominal height above the unprocessed surface of 10µm and a nominal width of 5µm as shown in Figure 1. While the recast material could have effectively been removed by additional laser processing, these features were left in place to aid hydrophobic performance.

Table 1. Laser parameters used for dimple textures on EN40 steel plate.

Ave. Power (w)	Pulse duration (ns)	Frequency (kHz)	Scan speed (mm/s)	Hatch size (µm)	NOP
6	100	60	1000	5	600

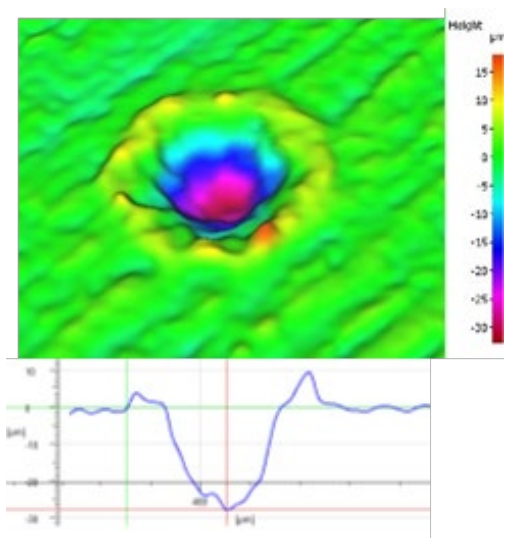

Fig. 1. Alicona 3-D image of a dimple feature in EN40 steel plate

2.2. Columnar texturing – femtosecond pulsed laser

Textures consisting of regular defined columnar frustums were created in flat Al plate using an AgieCharmilles P 400 U femtosecond pulsed laser system produced by Georg Fischer Machining Solutions. The laser source is a Satsuma fibre laser by Amplitude Systemes. The parameters employed to produce the textures using a line scan hatch strategy at angles of 0^0 and 90^0 are given in Table 2.

Table 2. Laser parameters used for dimple textures on Al plate.

Ave. Power (w)	Pulse duration (fs)	Frequency (kHz)	Speed (mm/s)	Hatch size (µm)	NOP
20	400	2	3000	10	100

The texture design consists of pyramids with a square base of 100µm x 100µm arranged in a grid pattern with a spacing of 100µm. The generated surfaces were analysed employing a SENSOFAR Smart apparatus using the confocal configuration at 10X magnification. Figure 2 shows a 3-D image of the prepared surfaces and Figure 3 shows the height profile taken from the pillar tops. The average height of the pillars was measured as 110µm.

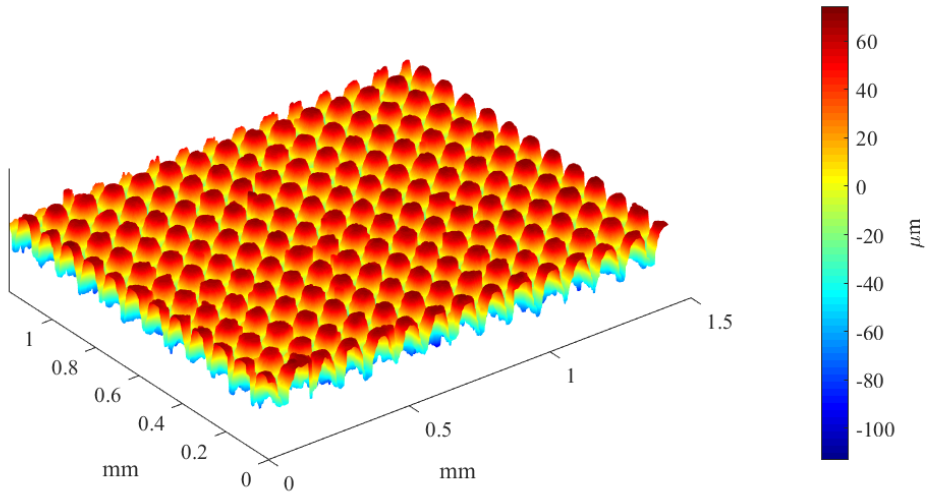

Fig. 2. 3-D image of a portion of the textured columnar surface

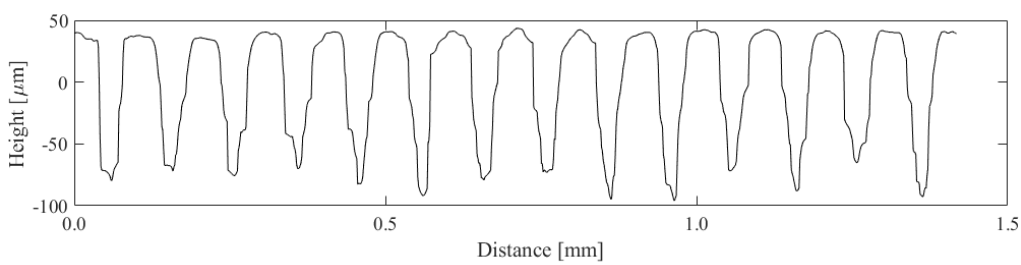

Fig. 3. Height profile along the columnar textured surface

3. Experimental methodology for hydrophobicity

3.1. Static droplet contact angle

The static water contact angle of the surface was characterised using a contact angle goniometer (FTA200, First Ten Angstroms), as shown in Figure 4. A water droplet was delivered onto the sample surface with pumping out rate of 1 µL/s and recorded by a CCD camera. The static water contact angle was obtained by Laplace-Young Fit method using the drop shape analysis software.

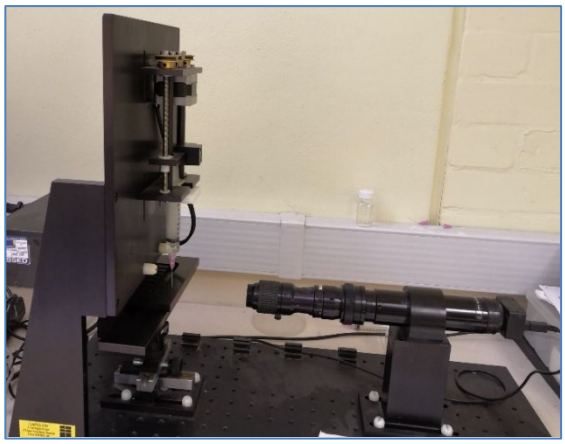

Fig. 4. Photographic image of the contact angle goniometer FTA 2000 arrangement

3.2. Tilted droplet contact angle

The sliding angle can be defined as the critical angle at which a droplet initiates mobility down an inclined surface by gradual tilting and is widely used to assess surface hydrophobicity as reported by Sakai et. al., 2009. Compared with the contact angle hysteresis, the sliding angle can be measured more easily and accurately to evaluate the mobility of the water droplet on the surface. A low sliding angle, the water droplet may enable a self-cleaning function of the surface as suggested by Hao, 2010.

The sliding angle of the samples was measured using a slope with an adjustable angle as shown in Figure 5. The sample was placed on top of the plate at the horizontal position and a water droplet was pumped on the sample surface. Subsequently, the scissor lift was continuously lifted until the droplet rolls. The angle of the slope at the rolling-off moment calculated by the following equation, which is considered as the sliding angle:

$$\alpha = \tan^{-1}\frac{H-h}{L} \qquad [3]$$

in which α is the sliding angle; h is the height of the fixed platform; H is the height of the scissor lift when the droplet rolls off; L is the distance between the two supporting points of the plate, as presented by Fu, 2017.

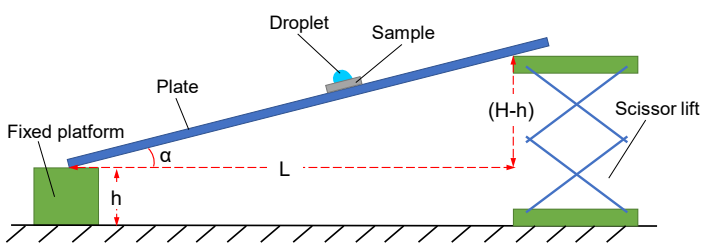

Fig. 5. Diagrammatic sketch of the sliding angle measurement, Fu, 2017

3.3. Accelerated aging

Accelerated surface aging provides a measure of the effects of changes to surface charge energy and chemical characteristics over a defined measurement period. Figure 6 shows the durability test rig setup, which is configured to use compressed air, gas propelled water droplets and/or SiC abrasives in suspension in water in a spray form directed onto a target surface. The accelerated aging test was set up to be performed for 20 minutes using a gas pressure of 15 psi, velocity of up to 37 m /s, at a flow of 20 L / min with a distance between the sample and the spray nozzle of 4 cm. The water contact angles were measured before and after the accelerated aging test.

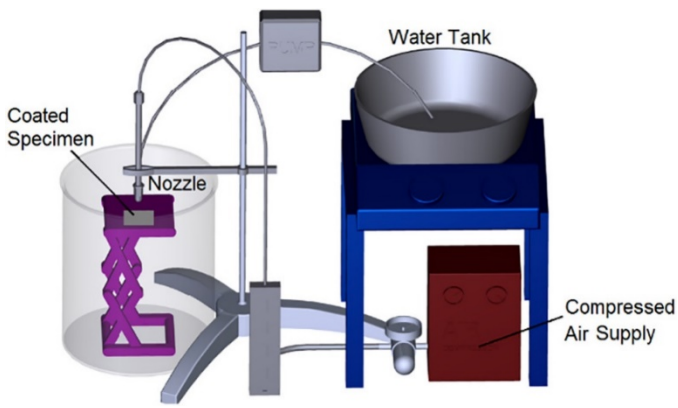

Fig. 6. Accelerated surface aging test apparatus

4. Results and discussion

4.1. Nanosecond pulsed laser produced dimpled textures

The laser dimpled patterned surfaces were each evaluated after rinsing in acetone followed with a laboratory grade isopropyl alcohol rinse and allowed to air dry. The laser textured surfaces were compared with a ground flat plate of identical material for reference. The results of the static water droplet contact angle captured using the experimental setup described in 3.1 are shown in Figure 7.

It can be seen from the image sequence that there is a distinct correlation with the dimpled area ratio and water droplet contact angle corresponding to 58.58^0 for the 5% area ratio, increasing to 139.58^0 for the 50% area ratio, the reference ground plate having improved hydrophobic performance to the plate having 5% dimpled area ratio.

While the produced dimples would allow air pockets to be trapped under incident water droplets and therefore contribute to the surfaces' hydrophobic performance, the resulting recast crown around the crater perimeters would also be expected to significantly contribute to the overall hydrophobic performance of the surfaces.

Although the control of hydrophobic performance of laser processed surfaces could be adequately demonstrated based on the texture design, the dimple structures produced with nanosecond pulsed laser did not reach superhydrophobic performance levels.

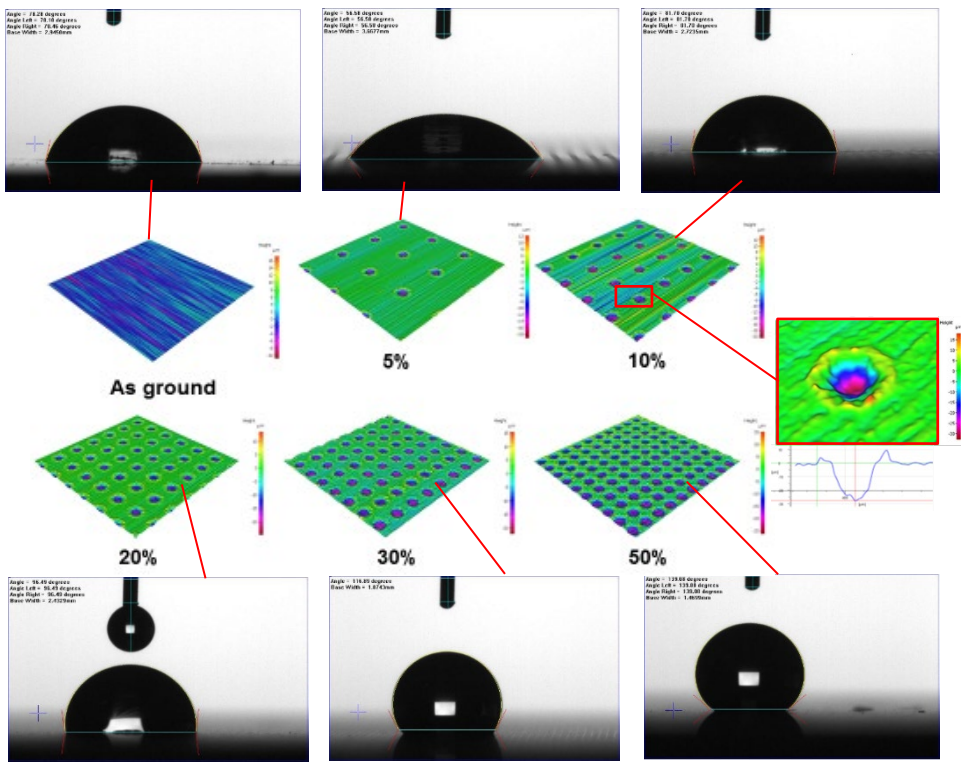

Fig. 7. Static water droplet contact angles of laser processed dimpled EN40 steel plates

4.2. Femtosecond pulsed laser produced columnar textures

A selected sample plate incorporating the femtosecond pulsed laser processed columnar pattern as described in 2.2 was evaluated for hydrophobic performance after carrying out the earlier described surface cleaning procedure. The static test results are shown in Figure 8.

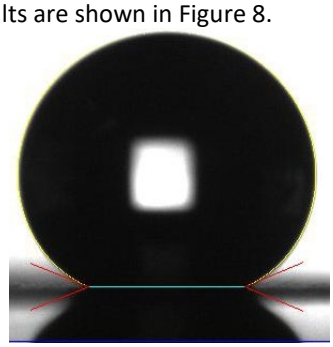

Fig. 8. Water droplet contact angle of 157^{o} on laser processed columnar pattened Al plate

The well-defined columnar geometry and the regular pattern produced by the femtosecond pulsed laser processing produced superhydrophobic performance when measured for the static water droplet contact angle as described in 3.1. Furthermore high droplet mobility was measured using the tilt angle test, producing mobility at a plate tilt of above 2^0. In addition results were consistent across the entire laser processed sites, indicating uniformity of the processed surface.

The accelerated aging test as described in 3.3 was applied for the duration of 20 minutes to selected processed samples in order to assess the stability and durability of its hydrophobic performance. In the case of the laser produced textures, an air blast was selected so as not to disturb or damage the as-processed surface during the accelerated aging test. The measured result revealed that the water droplet contact angle reduced significantly within the range shown in Figure 9.

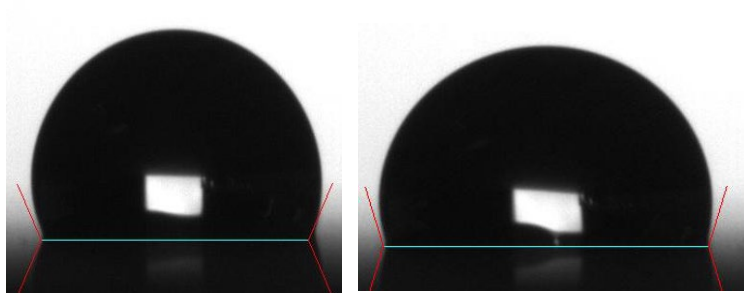

Fig. 9. Water droplet contact angles of 115^0 and 107^0 of laser processed columnar patterns after surface aging

It can be observed that the wetting contact angles decreased significantly and produced different values at sites across the selected surfaces after the aggressive aging, indicating that they no longer produced consistent superhydrophobic performance levels, highlighting the need for further surface processing.

5. Conclusions

It has been demonstrated in this study that laser processing is highly capable of producing textured surfaces which can produce controlled levels of hydrophobic performance, allowing textures to be designed for either local or wider sites on a surface to match the required performance levels of particular applications. While the nanosecond pulsed processing using near IR wavelength, produced dimpled features of controlled dimensions and spacing in hardened steel plate, secondary processing may be needed where high accuracy of feature geometry is required for such materials.

It has been further demonstrated that using ultra-fast (femtosecond) pulsed laser processing with a similar wavelength, textures containing well defined columnar micro-asperities having highly controlled geometries, protrusion/depth and spacing can be produced. Such textures produced on the surfaces of Al plate exhibited consistent superhydrophobic performance levels across the entire processed area.

It is the case for laser processed surfaces, like with other methods referenced in this study used to produce superhydrophobic surfaces, aging takes place after processing which affects the level hydrophobic performance over time. Nonetheless the study provides a significant platform on which subsequent processing can be developed to achieve long-term stability of hydrophobic performance of laser-processed surfaces.

References

Barthlott, W,, C. Neinhuis, C., 1997. Purity of the sacred lotus, or escape from contamination in biological surfaces, Planta, 202, 1, p. 1

Jungwirth, P., P.S. Cremer, P.S., 2014. Effects of the Hofmeister series of sodium salts on the solvent properties of water. Nature Chem. 6, p. 261

Wenzel, R.N., 1936. Resistance of solid surfaces to wetting by water. J. Ind. Eng. Chem. (Washington, D. C.), 28, p. 988

Cassie, A.D.B, Baxter, S., 1994. Wettability of porous surfaces. Trans. Faraday Soc., 40, 5, p. 546

Gao, L.C., Mccarthy, T.J., Zhang, X., 2009. Wetting and Superhydrophobicity. Langmuir, 25 (24), p. 14100

Extrand, C.W., Kumagai, Y., 1997. An Experimental Study of Contact Angle Hysteresis, J. Colloid Interface Sci.,191, 2, p. 378

Gao, L., Mccarthy, T.J., 2006. The Lotus Effect Explained: Two Reasons Why Two Length Scales of Topography Are Important," ACS J. Surf. & Coll., 22(7), p. 2966

Shirtcliffe, N.J., McHale, G., Atherton, S,. Newton, M.I., 2010. An introduction to superhydrophobicity, Adv. Colloid Interface Sci.,161, 1–2, p.124

Luo, B.H., Shum, P.W., Zhou, Z.F., K.Y. Li, K.Y., 2010. Preparation of hydrophobic surface on steel by patterning using laser ablation process, Surface & Coatings Technology, 204(8), p. 1180

Tang, M., Hong, M.H., Choo, Y.S., 2008. Hydrophobic Surface Fabrication by Laser Micro patterning, IEEE PhotonicsGlobal, Singapore, p. 1

Kietzig, A.M., Hatzikiriakos, S.G., Englezos, P., 2009. Patterned superhydrophobic metallic surfaces, Langmuir, 25, 8, p. 4821

Kim, M., Noh, J., 2018. Fabrication of a Hydrophilic Line on a Hydrophobic Surface by Laser Ablation Processing, National Library of Medicine. Micromachines, 9, p. I5.

Sakai, M., Kono, H., Nakajima, A., Zhang, X., Sakai, H., Abe, M., Fujishima, A., 2009. Sliding of water droplets on the superhydrophobic surface with ZnO nanorods, Langmuir, 25, p. 14182

Hao, P., Lv, C., Yao, Z., He, F., 2010. Sliding behavior of water droplet on superhydrophobic surface, EPL (Europhysics Letters) 90, p. 66003

Fu, Y., 2017. Development of Metallic-based Durable Superhydrophobic Surface, Master thesis, University of Nottingham, UK.